LETTER

doi:10.1038/nature12276

Attention enhances synaptic efficacy and the signal-to-noise ratio in neural circuits

Farran Briggs[1,2], George R. Mangun[3,4,5] & W. Martin Usrey[1,5,6]

Attention is a critical component of perception[1]. However, the mechanisms by which attention modulates neuronal communication to guide behaviour are poorly understood. To elucidate the synaptic mechanisms of attention, we developed a sensitive assay of attentional modulation of neuronal communication. In alert monkeys performing a visual spatial attention task, we probed thalamocortical communication by electrically stimulating neurons in the lateral geniculate nucleus of the thalamus while simultaneously recording shock-evoked responses from monosynaptically connected neurons in primary visual cortex. We found that attention enhances neuronal communication by increasing the efficacy of presynaptic input in driving postsynaptic responses, by increasing synchronous responses among ensembles of postsynaptic neurons receiving independent input, and by decreasing redundant signals between postsynaptic neurons receiving common input. The results demonstrate that attention finely tunes neuronal communication at the synaptic level by selectively altering synaptic weights, enabling enhanced detection of salient events in the noisy sensory environment.

Selective attention is a powerful brain mechanism that enables enhanced processing of relevant information while preventing interference from distracting events. Many studies in humans and animals have established that visual attention can influence sensory information processing in visual cortex[2–8] and subcortical visual areas[9–11]. Attention directed towards stimuli within the receptive field of a neuron in visual cortex generally results in increases in neuronal firing rate[12,13] and synchrony[14,15]. More recent work indicates that visual attention can also alter the correlation structure, variability and/or response gain of neuronal activity[14,16–18]. However, the fundamental mechanisms by which visual attention alters communication in neural circuits, at the synaptic level, remain a mystery. Moreover, it is unclear how attention-mediated alterations in neuronal population activity translate into improvements in perception[19].

To elucidate the synaptic mechanisms of attention, we developed a sensitive electrophysiological assay of neuronal communication involving stimulation of thalamocortical neurons in the lateral geniculate nucleus (LGN) of the thalamus and simultaneous recordings from monosynaptically connected (that is, postsynaptic) neurons in primary visual cortex (V1) of macaque monkeys performing a spatial attention task. First, we tested whether visual attention alters the efficacy of synaptic communication between the LGN and V1, defined here as the probability that presynaptic stimulation evokes a postsynaptic action potential. Second, we examined whether attention alters both signal and noise in correlated activity among ensembles of postsynaptic target neurons.

Two monkeys were trained to maintain central fixation while covertly focusing their attention on one of two drifting gratings in order to report a contrast change in the attended stimulus (Fig. 1). One of the gratings was positioned over the receptive fields of recorded neurons and the other was located at an equivalent eccentricity away from the receptive fields. Trials in which attention was directed towards (attend-towards condition) and away (attend-away condition) from the receptive fields of recorded neurons were organized into blocks and cued by the colour of the central fixation dot. In a random 5% of the trials the cue instruction was invalid, such that the contrast change occurred at the unattended location. Animals were rewarded for correct detection of the contrast change in validly and invalidly cued trials. Behavioural measures of spatial attention were derived by comparisons of accuracy (percentage of trials completed correctly) and reaction times in validly and invalidly cued trials. For both monkeys, accuracy was significantly greater ($P < 0.03$) and reaction times were significantly faster ($P < 0.05$; Fig. 1b) for validly versus invalidly cued trials, indicating that animals were covertly attending to the specified location.

In each animal, we implanted stimulating electrodes in the magnocellular and parvocellular layers of the LGN (Fig. 2a), so that weak electrical shocks applied to thalamocortical neurons in these layers evoked suprathreshold, short- and fixed-latency monosynaptic spikes in recorded (postsynaptic) thalamocortical-recipient (TCR) neurons, located in layer 4C of V1 (Fig. 2a, b). Importantly, stimulation levels were set so that stimulation evoked a postsynaptic spike in only a fraction of trials (Supplementary Fig. 1a). We recorded visually evoked activity in response to drifting sinusoidal gratings in order to characterize the physiological responses of all recorded TCR neurons. TCR neurons ($n = 61$) were grouped into those receiving input from the magnocellular layers and from the parvocellular layers (we refer to these as magnocellular-recipient ($n = 36$) and parvocellular-recipient ($n = 25$) populations, respectively) based on the stimulus contrast required to evoke a half-maximum response (Fig. 2c). Magnocellular- and parvocellular-recipient neurons differed across several physiological

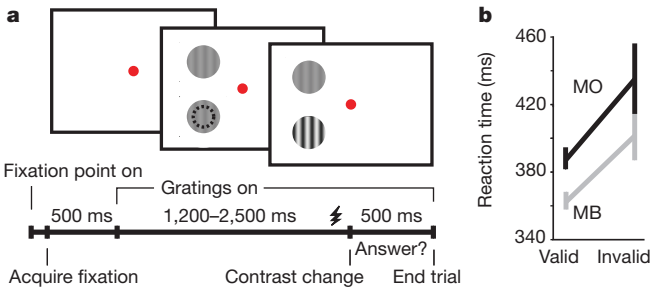

Figure 1 | Attention task and behavioural performance. a, The attention task, including representative frames of the visual display for a validly cued trial in which attention was directed by cue colour (the central fixation point; red in this case) towards the receptive field of the neuron. Dashed black circle (middle frame) represents the receptive field of the recorded neuron. The timeline for one trial is shown at bottom; LGN shock timing is indicated schematically just before the contrast change (shocks occurred on 70% of trials). **b**, Reaction time data for validly versus invalidly cued trials for the two monkeys (Monkey B (MB), $P < 0.01$; Monkey O (MO), $P < 0.05$). Error bars represent s.e.m.

[1]Center for Neuroscience, University of California, Davis, 1544 Newton Court, Davis, California 95618, USA. [2]Department of Physiology and Neurobiology, Geisel School of Medicine at Dartmouth, 1 Medical Center Drive, Lebanon, New Hampshire 03756, USA. [3]Center for Mind and Brain, University of California, Davis, 267 Cousteau Place, Davis, California 95618, USA. [4]Department of Psychology, University of California, Davis, 1 Shields Avenue, Davis, California 95616, USA. [5]Department of Neurology, University of California, Davis, 4860 Y Street, Sacramento, California 95817, USA. [6]Department of Neurobiology, Physiology and Behavior, University of California, Davis, 1 Shields Avenue, Davis, California 95616, USA.

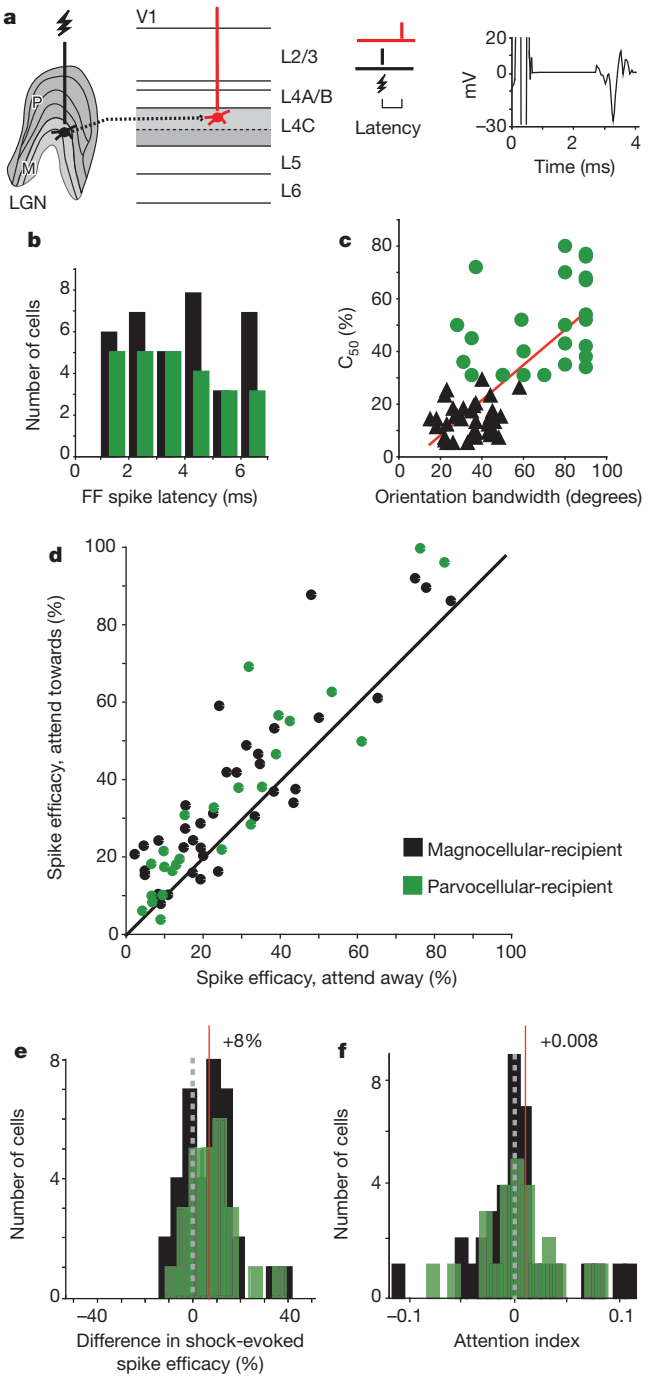

Figure 2 | Attentional modulation of thalamocortical synaptic efficacy. **a**, Experimental setup. Electrical stimulation of presynaptic LGN neurons (black) leads to a postsynaptic response in the simultaneously recorded TCR neuron (red). Shock-evoked postsynaptic spikes occur at fixed latencies with little temporal jitter, as illustrated by the trial-averaged waveform of a representative TCR neuron (right). **b**, Distribution of postsynaptic-response latencies for magnocellular- and parvocellular-recipient neurons in black and green, respectively (mean latency; magnocellular-recipient neurons $= 3.4 \pm 0.3$ ms, parvocellular-recipient neurons $= 3.1 \pm 0.4$ ms). FF, feedforward. **c**, Relationship between C_{50} (contrast for half-maximum response) and orientation-tuning bandwidth (peak half-width, at half height) for magnocellular- and parvocellular-recipient neurons ($R^2 = 0.52$). Magnocellular-recipient neurons; $C_{50} = 13.8 \pm 1.1\%$, orientation half-width $= 34 \pm 1.8^\circ$. Parvocellular-recipient neurons; $C_{50} = 49.4 \pm 3.4\%$, orientation half-width $= 69 \pm 4.6^\circ$. Colour conventions as in **b**. **d**, Percentage of shock-evoked postsynaptic spikes in attend-towards versus attend-away conditions. Black line represents unity. Average efficacy (percentage of shocks that evoke a postsynaptic response): for all TCRs, attend towards $= 36 \pm 3\%$, attend away $= 28 \pm 3\%$; magnocellular-recipient neurons, attend towards $= 37 \pm 4\%$, attend away $= 29 \pm 4\%$; parvocellular-recipient neurons, attend towards $= 35 \pm 5\%$, attend away $= 28 \pm 5\%$. **e**, **f**, Distributionsof differences in (**e**) shock-evoked spike efficacy (attend-towards versus attend-away condition) and (**f**) attention-index values for magnocellular- and parvocellular-recipient neurons (note difference in scales). Attention index values calculated from firing rate 850 to 1,200 ms after onset of grating stimulation. Dashed lines indicate zero and red lines indicate mean values (mean difference in spike efficacy for magnocellular- and parvocellular-recipient TCRs $= 8 \pm 2\%$; mean attention index magnocellular-recipient $= 0.008 \pm 0.007$, parvocellular-recipient $= 0.006 \pm 0.007$; colour conventions as in **b**.).

parameters, including orientation tuning ($P < 0.001$; Fig. 2c), the ratio of the first harmonic (f1; fundamental frequency) to mean response (f0; $P < 0.001$), and visually evoked firing rates ($P < 0.05$). However, shock efficacies (Supplementary Fig. 1a), spontaneous firing rates, and shock-evoked postsynaptic-response latencies (Fig. 2b) did not vary significantly across the magnocellular- and parvocellular-recipient populations, consistent with previous reports[20].

After TCR neurons were characterized physiologically, we recorded both visually evoked and shock-evoked neuronal responses while animals performed the attention task. In a subset of attention trials (70%), a single shock was delivered to the LGN between 1,000 and 1,200 ms after the onset of grating presentation, always at the same phase of the visual stimulus cycle, and before the contrast change. Electrical stimulation did not affect performance, as there was not a significant difference in the animals' ability to complete shock and non-shock trials in the attend-towards or attend-away conditions ($P > 0.5$). When we compared thalamocortical synaptic efficacy (per cent of presynaptic shocks that evoked a postsynaptic spike) as a function of attention, we observed a highly significant increase in synaptic efficacy when covert spatial attention was directed towards the receptive fields of recorded TCR neurons compared to when attention was directed away from TCR receptive fields ($P < 0.001$; Fig. 2d). Attentional modulation of synaptic efficacy was significant for both magnocellular- and parvocellular-recipient neuronal populations ($P < 0.001$ for both). For the attend-away trials, it is interesting to note that the number of spikes occurring within the time window corresponding to the postsynaptic response latency did not differ between shock and non-shock trials (Supplementary Fig. 1b), despite the fact that shock strength was set to be effective in neutral conditions. This finding is consistent with the view that attention may also have a suppressive influence on synaptic efficacy when directed away from a neuron's receptive field.

The robust attentional enhancement of thalamocortical synaptic efficacy, indexed by the positive shift in shock-evoked spike efficacy across attention conditions (Fig. 2e), contrasts with a modest attention-mediated increase in neuronal firing rate (Fig. 2f; statistically significant for magnocellular-recipient ($P < 0.025$), but not parvocellular-recipient ($P > 0.1$) neurons). Interestingly, this modest increase in firing rate across attention conditions was only evident for later time periods between stimulus onset and the earliest opportunity for contrast change (850 to 1,200 ms and 1,000 to 1,200 ms), and was not evident over earlier or broader time periods (0 to 1,200 ms or 600 to 1,200 ms; $P > 0.75$; Supplementary Fig. 1c), consistent with previous studies showing weak or no attentional modulation of firing rate in V1 (refs 7, 21–24). Further analysis also demonstrated that there was no relationship between the magnitude of attention effects on firing rate and the influence of attention on the efficacy of thalamocortical communication (Supplementary Fig. 1d). These results suggest that; first, attentional modulation of synaptic efficacy in thalamocortical circuits is not merely due to simple gain or firing-threshold changes in LGN or TCR neurons; and second, that thalamocortical visual pathways may make use of a different (synaptic-level) mechanism to propagate attentional signals compared to higher visual areas, where attentional modulation can be indexed by changes in neuronal firing rates.

We explored further the temporal precision of attentional modulation of synaptic efficacy in thalamocortical circuits by examining spiking

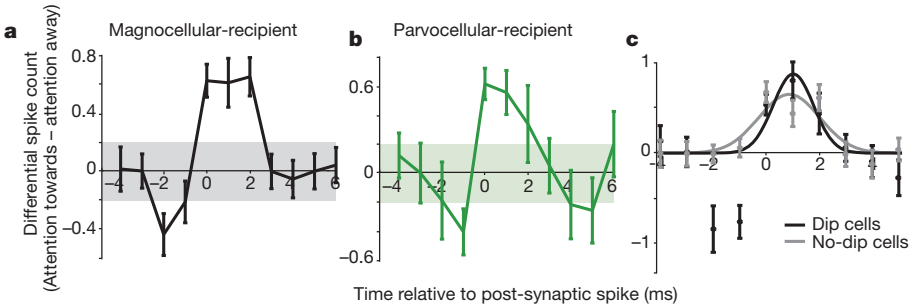

Figure 3 | Temporal precision of attentional enhancement of synaptic efficacy. **a**, **b**, Average differential spiking activity (attend towards—attend away) surrounding the time of the shock-evoked postsynaptic spike (occurring at time = 0) for magnocellular-recipient TCR neurons (**a**), and parvocellular-recipient TCR neurons (**b**). Error bars represent s.e.m.; shaded regions represent 2 s.d. above and below mean activity. **c**, Average differential spiking activity of TCR neurons separated into groups on the basis of whether they displayed early inhibition (dip versus no-dip cells). Error bars represent s.e.m. Black and grey lines illustrate Gaussian fits to dip and no-dip cell data. Width at half height for dip cells = 1.75 ms; for no-dip cells = 2.75 ms.

activity over a 10-ms window surrounding the time of the shock-evoked postsynaptic spike (–4 ms to +6 ms). Figure 3a, b illustrates the population average time-course of differential spiking activity (attend towards–attend away) surrounding the shock-evoked postsynaptic spike (defined as time = 0) for magnocellular- and parvocellular-recipient neurons, respectively (see Supplementary Fig. 2a for separate time-course plots corresponding to each attention condition). In both cases, spiking activity rises above two standard deviations of the mean activity for 2 to 3 ms, indicating that attention causes an increase in the number of synaptically evoked spikes during a limited time window. Notably, about 40% of TCR neurons (42% of magnocellular-recipient neurons, and 40% of parvocellular-recipient neurons) displayed a prominent dip in spiking activity just before the evoked spike (Fig. 3a, b and Supplementary Fig. 2a, b), suggesting that fast feedforward inhibition, probably via local interneurons, may suppress spiking activity just before the occurrence of the postsynaptically evoked spike. Consistent with this, we found that TCR subpopulations with fast feedforward inhibition showed less jitter in the timing of their shock-evoked postsynaptic spikes (response profile = 1.75 ms for 'dip' neurons versus 2.75 ms for 'no-dip' neurons; Fig. 3c). These results suggest that feedforward inhibition sharpens postsynaptic spike-timing precision by approximately 1 ms. The presence of dips illustrates that attentional modulation in our sample of V1 neurons was often dynamic, including phases of reduced spiking as well as phases of increased spiking. These dynamics could help to explain why attentional modulation did not produce a larger increase in overall firing rate.

After it was established that attention alters the efficacy of synaptic communication in neural circuits with fine temporal precision, we next set out to determine whether attention differentially affects the processing of signal and noise in thalamocortical circuits. Previous studies have provided evidence to suggest that attention may alter neuronal activity by increasing signal or reducing noise in firing-rate fluctuations[20,22]. We assessed whether attention could both boost the signal and reduce noise in the same circuit by examining the effects of attention on the occurrence of synchronized spikes between pairs of simultaneously recorded TCR neurons. In some circumstances, synchronized spiking may boost signal detection by driving downstream targets more effectively[25,26], whereas in other cases, synchronized spiking may confound decoding by downstream target neurons through the introduction of noise[27]. Using a multi-electrode recording array, we recorded from 71 pairs of simultaneously recorded TCR neurons that fired synchronized spikes in response to electrical stimulation in the LGN. Our criteria for identifying synchronous postsynaptic spikes were strict: in any given trial, synchronous spikes needed to occur at the specified shock-evoked postsynaptic spike latencies for each TCR neuron in the pair. For each pair, we calculated the percentage of trials in which synchronous spikes were evoked in response to electrical stimulation in the attend-towards versus attend-away conditions. Results from this analysis were clear; attention significantly increased the percentage of synchronous spikes across our sample of TCR pairs (Fig. 4a, b; $P < 0.001$). This effect was present for magnocellular–magnocellular, parvocellular–parvocellular, and magnocellular–parvocellular pairs in our sample ($P < 0.04$; Fig. 4a, b, black, green and grey symbols, respectively), suggesting that attentional modulation of spike synchrony is consistent across thalamocortical circuits.

Synchronized spiking between pairs of TCR neurons could arise from two sources: first, the simultaneous arrival of spikes travelling in independent channels of communication (for example, different LGN axons); and second, the simultaneous arrival of spikes travelling in a common channel (for example, one LGN axon) with divergence. Although both mechanisms will propagate signal (stimulus-evoked) and noise spikes to their postsynaptic targets, randomly generated noise spikes are less likely to occur simultaneously between independent LGN axons than between the branches of common input LGN axons. Consequently, attention could increase the ratio of signal-to-noise in thalamocortical circuits by increasing the strength of spikes arriving from independent channels, and also by reducing the strength of spikes arriving from common-input channels. To determine whether pairs of TCR neurons in our sample received common LGN input, we calculated shuffle-corrected cross-correlograms from TCR neuronal responses to drifting sinusoidal gratings. For 25 TCR pairs, cross-correlograms contained a single, narrow (<3 ms, full width at half height) peak centred at time zero, indicating that the two neurons frequently fired synchronous spikes in response to common feedforward input (Fig. 4c). TCR pairs in our sample with zero-centred cross-correlogram peaks had overlapping receptive fields, consistent with previous studies of correlation patterns shown by visual neurons with common feedforward input[26]. Most recorded TCR pairs consisted of two magnocellular-recipient neurons or two parvocellular-recipient neurons, consistent with the anatomical segregation of magnocellular and parvocellular inputs to V1. However, we also encountered pairs of mixed magnocellular- and parvocellular-recipient neurons.

For TCR pairs receiving common input, we calculated the percentage of synchronous spikes (that is, the percentage of spikes contained in the cross-correlogram peak) when attention was directed towards and away from the cells' receptive fields. Results of this analysis showed that attention decreased the percentage of synchronous spikes from common input by approximately10% (see Supplementary Methods). Consistent with this, the distribution of differential cross-correlogram peak height (attend towards–attend away) was shifted significantly to the left of zero ($P < 0.01$), indicating that attention decreased synchronous responses to common input (Fig. 4d). These results suggest that attention may decrease noise in thalamocortical communication by reducing the amount of synchronous spikes arising from common feedforward input.

As a final analysis, we explored whether attention differentially modulated synchronous spiking in pairs of TCR neurons receiving input from independent sources (that is, TCR pairs with flat cross-correlograms)

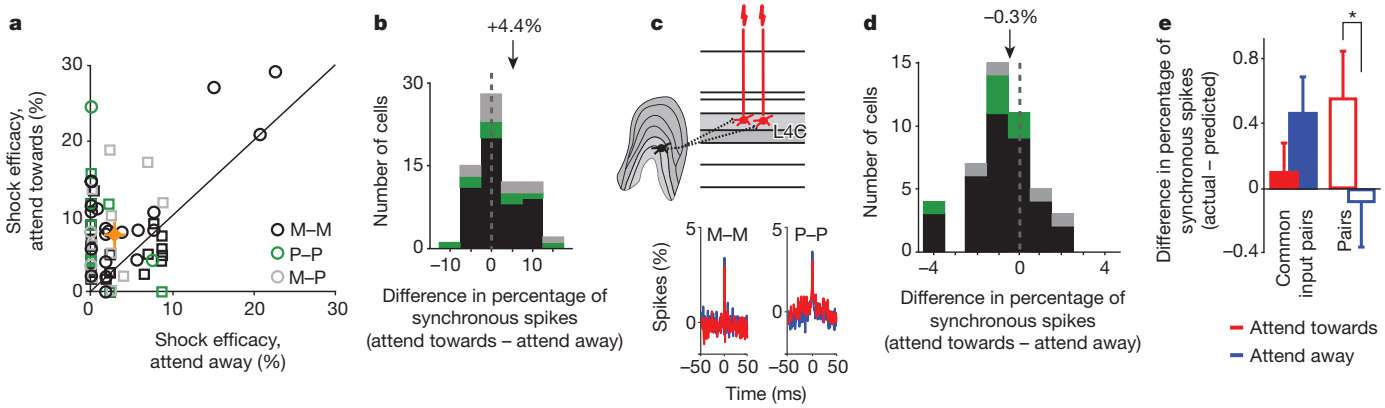

Figure 4 | Attentional modulation of synchronized spiking. **a**, The efficacy of shocks in evoking synchronous spikes; the percentage of synchronously evoked postsynaptic spikes across attention conditions for 71 pairs of simultaneously recorded magnocellular–magnocellular (M–M; black, $n = 48$), parvocellular–parvocellular (P–P; green, $n = 11$), magnocellular–parvocellular (M–P; grey, $n = 12$) TCR pairs (circles represent TCR pairs; squares represent putative TCR pairs). Black line represents unity. Average efficacy of synchronous spiking across all pairs in the attend-towards condition $= 7.6 \pm 0.8\%$, and in the attend-away condition $= 3.1 \pm 0.6\%$ (orange diamond, cross-hairs represent s.e.m.). **b**, Distribution of attention-mediated differences in the percentage of shock-evoked synchronous spikes. Colour conventions as in **a**. Dashed line represents zero and arrow illustrates the population mean ($+4.4 \pm 0.7\%$ s.e.m.). **c**, Diagram illustrating a pair of TCR neurons receiving common presynaptic input and two examples of shuffle-corrected cross-correlograms for magnocellular–magnocellular-recipient and parvocellular–parvocellular-recipient pairs, illustrating the occurrence of synchronous spikes (narrow peaks centred at time zero) and the influence of attention on the percentage of synchronous spikes in attend-towards (red) and attend-away (blue) conditions. **d**, Distribution of attention-mediated differences in correlated spikes among pairs receiving common input (21 magnocellular–magnocellular, 2 parvocellular–parvocellular, and 2 magnocellular–parvocellular pairs). Conventions as in **b**. Mean difference in spikes in peak $= -0.3 \pm 0.2\%$. **e**, Difference between actual and predicted synchronous spikes for TCR pairs receiving common feedforward input (solid bars; $n = 25$) and TCR pairs receiving independent input (open bars; $n = 46$) across attention conditions. Error bars represent s.e.m.; asterisk indicates significant difference across attention conditions for TCR pairs receiving independent input ($P < 0.025$). Average actual − predicted values: common input TCR pairs, attend towards $= 0.1 \pm 0.2\%$, attend away $= 0.5 \pm 0.2\%$; independent input TCR pairs, attend towards $= 0.6 \pm 0.3\%$, attend away $= -0.1 \pm 0.3\%$.

compared to TCR pairs that received input from common sources (that is, TCR pairs with narrow, zero-centred cross-correlogram peaks). More specifically, we determined whether measured percentages of synchronous spikes differed from predicted percentages based on the product of the evoked postsynaptic spike probabilities measured for each TCR neuron in the pair (Fig. 4e). For TCR neurons receiving common input, the percentage of measured synchronous spikes was not significantly different from the prediction ($P > 0.25$), and there was no effect of attention on this relationship. However, for TCR pairs receiving independent input, there was a significant difference between actual and predicted synchronous spikes, and attention had a significant effect on the relationship between measured and predicted values ($P < 0.025$). These results suggest that attention differentially regulates synchronized inputs emerging from independent and common sources. Accordingly, attention boosts signal transmission by enhancing responses to synchronous inputs from independent sources and reduces noise transmission by reducing responses to synchronous inputs from common input sources. Based on our data, attention may boost signal-to-noise ratios on average by approximately 20% (see Methods). This finding has significant implications for understanding the mechanisms by which neural networks optimally encode sensory information in the face of potentially noisy correlations resulting from anatomical wiring constraints[27].

Taken together, the results of this study provide multiple insights into the mechanisms by which attention alters neuronal communication. First, attention modulates signal transmission by enhancing synaptic efficacy. This finding represents the first evidence that attention acts at the synaptic level. Second, attention modulates afferent signal transmission with fine temporal precision. Third, attention serves to increase the ratio of signal to noise in neural circuits by simultaneously enhancing the transmission of signal and reducing the transmission of noise. These results suggest strongly that attention modulates synaptic inputs in a highly selective manner, such that inputs that carry salient sensory information (through independent channels) are enhanced and inputs carrying potentially redundant information (through common channels) are suppressed. Each of these results has significant implications for our understanding of attentional modulation of sensory information processing.

Attentional modulation of synaptic efficacy in thalamocortical circuits was robust and displayed temporal precision. Attention-related improvements in spike-timing precision in V1 resulted in part from fast disynaptic feedforward inhibition. Interestingly, the temporal precision of attentional modulation of V1 activity did not correlate strongly with more global changes in firing rate (represented by an attention index calculated from peri-stimulus spiking activity). This lack of correspondence suggests that attention alters brain activity through multiple mechanisms, including more global alterations in neuronal firing rate, as well as finer-scale dynamic alterations in synaptic communication operating at the level of individual neural circuits. Moreover, our results support the idea that attentional modulations involving fine-scale dynamics may not manifest in more global alterations in neuronal firing rate. At the local circuit level, this effect may serve to enhance spatial and temporal precision, but at the more global level, these effects may average out. In V1 (and other sensory cortices), attention may make use of fine-scale dynamics to accommodate depressing synapses, a known property of thalamocortical afferents[28]. It would be interesting to know whether or not attention affects synaptic weights in higher visual cortical areas and, if so, whether the effects of attention on synaptic weights underlie the influence of attention on neuronal firing-rate dynamics.

Our data support the idea that attention enhances sensory information processing directly by increasing the ratio of signal to noise in neural-circuit communication. Simultaneous signal enhancement and noise reduction in the same neural circuit suggests that attention modulates correlated synaptic activity in a highly selective manner. Select synaptic connections that originate from independent inputs and carrying feature-specific information about a sensory stimulus are more strongly weighted with attention, leading to better processing of salient stimulus features by downstream neurons. Synaptic connections that originate from common inputs are weighted less with attention, so that false positives are less likely to be communicated to downstream decoding neurons. Such asymmetric synaptic weighting with

attention hints at a presynaptic locus for modulation, because a postsynaptic locus, such as altering the membrane potential threshold of cortical recipient neurons, would be difficult to reconcile with asymmetric synaptic weights. Furthermore, the finding that attention does not increase the overall firing rate of cortical neurons that receive direct LGN input indicates that the measured changes in thalamocortical communication are unlikely to be due to a generalized depolarization among target neurons with attention. To determine the structural basis for presynaptic modulation is beyond the scope of the current study, but one possible candidate is differential modulation by acetylcholine. Acetylcholine has been implicated in attention effects in V1 (ref. 29), and a particular class of cholinergic receptors are localized to the presynaptic terminals of LGN axons that innervate cortical layer 4C neurons[30]. These cholinergic synapses could therefore provide a route for attention to alter synaptic weights selectively.

Feedforward subcortical–cortical and cortico–cortical connections often must convey information with speed and precision, but anatomical wiring constraints on these connections can introduce unreliable information. Here we demonstrate that attention alters synaptic communication in a dynamic and highly selective manner that could be uniquely adapted for signal transmission in sensory cortex. Specifically, attention selectively enhances inputs carrying salient sensory information while simultaneously suppressing inputs carrying potentially redundant information. These findings suggest that attention could represent a critical mechanism by which anatomical wiring limitations are overcome in order to optimize communication across neural circuits, thereby permitting the most behaviourally relevant information to influence perception and performance.

METHODS SUMMARY

Two adult female macaque monkeys (*Macacca mulatta*) were used for this study. All of the procedures carried out as a part of this study conformed to the guidelines set by the National Institutes of Health and were approved by the Institutional Animal Care and Use Committee at the University of California, Davis. Under full surgical anaesthesia, animals were implanted with head-posts and cylinders encircling two craniotomies over the LGN and V1. Animals learned a contrast-change detection task requiring covert shifts in visual spatial attention. Stimulating electrodes were semi-chronically implanted within the LGN and recording electrodes were placed in retinotopically aligned regions of V1. V1 neurons monosynaptically connected to LGN inputs were identified by short, fixed-latency action potentials after electrical stimulation of LGN neurons. Responses of (postsynaptic) thalamocortical-recipient (TCR) neurons in V1 to visual stimulation during trials in which animals' directed attention towards or away from drifting sinusoidal gratings placed within recorded neurons' receptive fields were compared. Electrical shocks were delivered to the LGN on a proportion of attention trials and the probability of a shock evoking a spike in TCR neurons was compared across attention conditions. Single-unit recordings of TCR neurons were made with single electrodes and a five-channel multi-electrode array. Spikes were sorted offline using principle components analysis. Subsequent data analyses included calculations of tuning responses in order to classify TCR neurons as receiving magnocellular or parvocellular LGN input, calculations of attention-index values, determination of shock-evoked spiking probability, and calculation of shuffle-corrected cross-correlograms for all simultaneously recorded pairs of TCR neurons.

Full Methods and any associated references are available in the online version of the paper.

Received 15 February; accepted 9 May 2013.
Published online 26 June 2013.

1. Posner, M. I., Synder, C. R. R. & Davidson, B. J. Attention and the detection of signals. *J. Exp. Psychol.* **109,** 160–174 (1980).
2. Van Voorhis, S. & Hillyard, S. A. Visual evoked potentials and selective attention to points in space. *Percept. Psychophys.* **22,** 54–62 (1977).
3. Moran, J. & Desimone, R. Selective attention gates visual processing in the extrastriate cortex. *Science* **229,** 782–784 (1985).
4. Heinze, H. J. *et al.* Combined spatial and temporal imaging of brain activity during visual selective attention in humans. *Nature* **372,** 543–546 (1994).
5. Ito, M. & Gilbert, C. D. Attention modulates contextual influences in the primary visual cortex of alert monkeys. *Neuron* **22,** 593–604 (1999).
6. Kelly, S. P., Gomez-Ramirez, M. & Foxe, J. J. Spatial attention modulates initial afferent activity in human primary visual cortex. *Cereb. Cortex* **18,** 2629–2636 (2008).
7. McAdams, C. J. & Reid, R. C. Attention modulates the responses of simple cells in monkey primary visual cortex. *J. Neurosci.* **25,** 11023–11033 (2005).
8. Thiele, A., Pooresmaeili, A., Delicato, L. S., Herrero, J. L. & Roelfsema, P. R. Additive effects of attention and stimulus contrast in primary visual cortex. *Cereb. Cortex* **19,** 2970–2981 (2009).
9. Vanduffel, W., Tootell, R. B. & Orban, G. A. Attention-dependent suppression of metabolic activity in the early stages of the macaque visual system. *Cereb. Cortex* **10,** 109–126 (2000).
10. O'Connor, D. H., Fukui, M. M., Pinsk, M. A. & Kastner, S. Attention modulates responses in the human lateral geniculate nucleus. *Nature Neurosci.* **5,** 1203–1209 (2002).
11. McAlonan, K., Cavanaugh, J. & Wurtz, R. H. Guarding the gateway to cortex with attention in visual thalamus. *Nature* **456,** 391–394 (2008).
12. Spitzer, H., Desimone, R. & Moran, J. Increased attention enhances both behavioral and neuronal performance. *Science* **240,** 338–340 (1988).
13. McAdams, C. J. & Maunsell, J. H. Attention to both space and feature modulates neuronal responses in macaque area V4. *J. Neurophysiol.* **83,** 1751–1755 (2000).
14. Fries, P., Reynolds, J. H., Rorie, A. E. & Desimone, R. Modulation of oscillatory neuronal synchronization by selective visual attention. *Science* **291,** 1560–1563 (2001).
15. Lakatos, P., Karmos, G., Mehta, A. D., Ulbert, I. & Schroeder, C. E. Entrainment of neuronal oscillations as a mechanism of attentional selection. *Science* **320,** 110–113 (2008).
16. Cohen, M. R. & Maunsell, J. H. Attention improves performance primarily by reducing interneuronal correlations. *Nature Neurosci.* **12,** 1594–1600 (2009).
17. Mitchell, J. F., Sundberg, K. A. & Reynolds, J. H. Spatial attention decorrelates intrinsic activity fluctuations in macaque area V4. *Neuron* **63,** 879–888 (2009).
18. Pestilli, F., Carrasco, M., Heeger, D. J. & Gardner, J. L. Attentional enhancement via selection and pooling of early sensory responses in human visual cortex. *Neuron* **72,** 832–846 (2011).
19. Zénon, A. & Krauzlis, R. J. Attention deficits without cortical neuronal deficits. *Nature* **489,** 434–437 (2012).
20. Bullier, J. & Henry, G. H. Ordinal position and afferent input of neurons in monkey striate cortex. *J. Comp. Neurol.* **193,** 913–935 (1980).
21. Chen, Y. *et al.* Task difficulty modulates the activity of specific neuronal populations in primary visual cortex. *Nature Neurosci.* **11,** 974–982 (2008).
22. Luck, S. J., Chelazzi, L., Hillyard, S. A. & Desimone, R. Neural mechanisms of spatial selective attention in area V1, V2, and V4 of macaque visual cortex. *J. Neurophysiol.* **77,** 24–42 (1997).
23. Motter, B. C. Focal attention produces spatially selective processing in visual cortical areas V1, V2, and V4 in the presence of competing stimuli. *J. Neurophysiol.* **70,** 909–919 (1993).
24. Yoshor, D., Ghose, G. M., Bosking, W. H., Sun, P. & Maunsell, J. H. R. Spatial attention does not strongly modulate neuronal responses in early human visual cortex. *J. Neurosci.* **27,** 13205–13209 (2007).
25. Usrey, W. M. The role of spike timing for thalamocortical processing. *Curr. Opin. Neurobiol.* **12,** 411–417 (2002).
26. Usrey, W. M., Alonso, J.-M. & Reid, R. C. Synaptic interactions between thalamic inputs to simple cells in cat visual cortex. *J. Neurosci.* **20,** 5461–5467 (2000).
27. Zohary, E., Shadlen, M. N. & Newsome, W. T. Correlated neuronal discharge rate and its implications for psychophysical performance. *Nature* **370,** 140–143 (1994).
28. Stratford, K. J., Tarczy-Hornoch, K., Martin, K. A. C., Bannister, N. J. & Jack, J. J. B. Excitatory synaptic inputs to spiny stellate cells in cat visual cortex. *Nature* **382,** 258–261 (1996).
29. Herrero, J. L. *et al.* Acetylcholine contributes through muscarinic receptors to attentional modulation in V1. *Nature* **454,** 1110–1114 (2008).
30. Disney, A. A., Aoki, C. & Hawken, M. J. Gain modulation by nicotine in macaque V1. *Neuron* **56,** 701–713 (2007).

Supplementary Information is available in the online version of the paper.

Acknowledgements We thank K. E. Neverkovec, D. J. Sperka and R. Oates-O'Brien for technical and veterinary assistance. This work was supported by National Institutes of Health grants EY18683 (F.B.), EY013588 (W.M.U.), MH055714 (G.R.M.) and NSF grants BCS-0727115 and 1228535 (G.R.M. and W.M.U.).

Author Contributions F.B., G.R.M. and W.M.U. designed the experiments. F.B. conducted the experiments and performed the data analyses in collaboration with G.R.M. and W.M.U. F.B., G.R.M. and W.M.U. wrote the manuscript.

Author Information Reprints and permissions information is available at www.nature.com/reprints. The authors declare no competing financial interests. Readers are welcome to comment on the online version of the paper. Correspondence and requests for materials should be addressed to W.M.U. (wmusrey@ucdavis.edu).

METHODS

Two adult female macaque monkeys (*Macacca mulatta*) were used for this study. All of the procedures performed as part of this study conformed to the guidelines set by the NIH and were approved by the Institutional Animal Care and Use Committee at the University of California, Davis.

Surgical preparation. All surgical procedures have been described in detail previously[31,32]. Under full surgical anaesthesia, two craniotomies were made to enable recording access to the LGN and to the parafoveal opercular region of V1. Two recording cylinders were placed encircling the craniotomies and incased in an implant of bone cement. Head-restraint posts were also attached to cranial implants. After recovery from surgery, cylinders were flushed with sterile saline plus providone-iodine (Butler Schein) or chlorhexidine at least three times per week. Treatment with 5-fluorouracil, and occasional dura scrapes, were performed weekly to maintain thin and healthy dura for ease of electrode penetration.

Visual stimulation. Visual stimuli were generated using a VSG/5 system (Cambridge Research Systems). Stimuli were presented on a gamma-calibrated Sony monitor placed 700 mm in front of animals' eyes. The refresh rate of the monitor was 140 Hz and the mean luminance was 38 cd m^{-2}. The monitor was the sole source of illumination in the room containing the animal. All stimuli were presented under binocular viewing conditions.

Behavioural training. Animals were trained to perform fixation and contrast-change detection tasks for juice rewards using standard operant conditioning. Eye position was monitored by an infrared video eye tracker (Applied Science Laboratories) with a refresh rate of 240 Hz. If animals' eye positions deviated by more than 0.35° at any point during a task trial, the trial was aborted. Fixation tasks required animals to maintain central fixation on a dot while drifting gratings were placed within the receptive fields of recorded neurons in order to measure neuronal visual physiology. For fixation tasks, trials were interleaved with a minimum 1-s period during which the monitor was mean luminance grey and animals were allowed to move their eyes freely.

Attention task. Animals were trained to detect a contrast change in one of two gratings and report the change using a joystick. Fixation was maintained throughout the duration of the trial, including the answer window. Animals were instructed to attend either to a drifting sinusoidal grating presented within (attend-towards condition) or an identical grating presented outside (attend-away condition) the receptive fields of the recorded neurons (Fig. 1a). The two gratings were identical and set to the orientation and spatial-frequency preference of the recorded neurons, and were always placed at an equal distance from the central fixation dot. Attention trials were run in blocks of 10 trials of each attention condition (attend towards or attend away) and the colour of the central fixation dot provided a cue to the animals, of where to allocate their attention. Trials progressed as follows. Trials were separated by a minimum of 1,000-ms, during which time the luminance of the monitor was maintained at background levels (mean luminance grey) and the animals were allowed to move their eyes freely, after which the monkeys could initiate a new trial by moving a joystick from the centre position to a side position (left or right of centre). Animals were required to maintain the joystick in the side position throughout the duration of the trial until the answer period; premature joystick movements caused trials to abort. After initial movement of the joystick to the side, a central fixation dot was displayed, to which animals directed their gaze. Five-hundred milliseconds after the onset of central fixation, two gratings appeared on the monitor, one inside and one outside the receptive field of recorded neurons. The two gratings were presented for a variable amount of time, between 1,200 and 2,500 ms, determined on a trial-by-trial basis according to a hazard function, with a mean at 1,700 ms. Following the period of visual stimulation by drifting gratings as determined by the hazard function, one of the two gratings increased in contrast by 10%. Both gratings remained on the monitor during a 500-ms answer window in which animals signalled detection of the contrast change by moving the joystick to the original central position. Only correct detection of the contrast change, indicated by a correct joystick movement, while also maintaining central gaze fixation throughout the answer period, was rewarded with juice. Trained animals typically performed with a success rate of 70% or above, discounting aborted trials. Trials were aborted when animals moved their eyes by more than 0.35° during any part of the trial or made a joystick movement before the contrast change. We found no significant differences in the proportion of aborted trials across attention conditions or across shock and non-shock trials ($P > 0.5$). Importantly, before the contrast change, visual stimulation was equal across attention conditions such that the only variable across conditions was the location to which the animal directed covert spatial attention.

Across blocks of trials, 95% of total trials were cued validly, wherein the contrast change occurred at the attended location signified by the colour of the fixation dot. In the remaining 5% of trials, the fixation dot colour cue was invalid and the contrast change occurred at the unattended location. Reaction times were measured as the time between the contrast change and movement of the joystick back to the central position. For each animal, reaction times were compared across validly and invalidly cued trials. Reaction time data were computed for all sessions including at least 50 correct trials in each attention condition (attend towards and attend away). Reaction time values were: monkey B, reaction time (valid) = 363 ± 5 ms, reaction time (invalid) = 401 ± 14 ms (monkey B, $P < 0.01$); monkey O, reaction time (valid) = 387 ± 7 ms, reaction time (invalid) = 435 ± 21 ms (monkey O, $P < 0.05$). In addition, both monkeys correctly detected grating contrast changes significantly more often in validly compared to invalidly cued trials ($P < 0.03$).

Electrical stimulation. As described in detail previously[31,32], stimulating electrodes were semi-chronically implanted within parafoveal regions of the LGN. Stimulating electrodes were placed in precise retinotopic alignment with recording electrodes in V1, such that receptive fields of neurons at each location were within less than 2° of one another in visual space. Single platinum or iridium stimulating electrodes (FHC) with less than 1 mm of tip exposure were placed within the LGN such that both magnocellular and parvocellular thalamocortical neuronal populations were activated. Placement of stimulating electrodes was guided and verified by recording visual responses from LGN neurons during and after implantation. Stimulation was generated by an isolated pulse stimulator (AM Systems) and included a single, brief (0.2-ms), biphasic current pulse (approximately 10 to 200 μA) delivered once every 5 s during collision testing (described below) and once per shock trial in the attention task (described below).

To locate putative TCR neurons, V1 recording electrodes were advanced slowly while shocks were delivered at regular intervals (every 5 s). TCR neurons were identified by the presence of short-latency (less than 6 ms) feedforward postsynaptic spikes in both collision and non-collision modes of stimulation, as described in detail previously[31,32]. Shock-evoked postsynaptic spike latencies were calculated as the time between the shock in the LGN and the postsynaptic spike. Magnocellular- and parvocellular-recipient neurons did not differ in their postsynaptic spike latencies (Fig. 2b; $P > 0.5$).

Collision testing was carried out to distinguish whether or not cortical neurons were activated by the arrival of orthodromically or antidromically propagated spikes after electrical stimulation. Collision tests were performed while the animals performed fixation tasks, or when they were free to move their eyes and the monitor was mean luminance grey. Shock current was set so that shocks evoked spikes approximately 35% of the time, on average, regardless of the behavioural condition or stimulus display. It was important to titrate the shock current for each individual TCR neuron such that shock-evoked postsynaptic spikes occurred on a fraction of trials in order to avoid floor or ceiling effects in the attention experiment. In 76 out of 80 recording sessions, shock strength was held constant across collision and attention testing conditions; in four sessions, shock strength was decreased for attention trials relative to collision trials.

Electrical stimulation during the attention task. In 70% of attention trials, a single shock (parameters as above, current set per TCR neuron) was delivered between 1,000 and 1,200 ms after the onset of the two drifting sinusoidal stimuli and before the contrast change. Shocks occurred at the same time in the stimulus cycle for both attend-towards and attend-away trials. The precise timing of the shock was set to match the neuron's peak response to the periodic stimulus. In this way, electrical stimulation occurred while the recorded neuron was excited (rather than suppressed) by the visual stimulus. Shocks were delivered towards the end of the visual stimulation period because animals' reaction times decreased systematically with increasing visual stimulation duration, suggesting that animals exerted greater attention towards the end of each trial (data not shown).

The efficacy of shocks in evoking postsynaptic spikes was determined for each TCR neuron based on all shock trials in the attention task, including attend-towards and attend-away trials (Supplementary Fig. 1a). Magnocellular- and parvocellular-recipient neurons did not differ in their shock-evoked spike efficacies (Supplementary Fig. 1a; $P > 0.05$).

Animals did not make voluntary or involuntary eye movements in response to electrical stimulation of the LGN (which would have resulted in aborted trials, as shocks occurred before grating-contrast changes), and electrical stimulation did not affect performance on the attention task. As electrical stimulation parameters were reduced such that the average efficacy of shock-evoked postsynaptic spikes was approximately 35%, and because the same proportion of trials included shocks in both attention conditions, it is unlikely that shocks induced visual percepts that interfered with animals' behaviour or changes in neuronal responses across attention conditions.

Electrophysiological recordings. Recordings from V1 neurons were made using single platinum-in-glass electrodes (Alpha Omega) or a Mini Matrix multi-electrode array of five platinum-in-quartz electrodes (Thomas Recording). Spiking data were amplified and recorded by a PC equipped with a Power 1401 acquisition system and Spike2 software package (Cambridge Electronic Design). For each recording session, the first step was the identification of putative TCR neurons

(described above). The second step involved characterizing the visual physiology of recorded neurons. This was accomplished by presenting drifting sinusoidal gratings that varied in orientation, contrast, spatial frequency or size within the centre of the receptive field while animals performed the fixation task. Gratings were presented for 1 to 2 s per trial, and trials were repeated at least two times. To generate response functions for orientation (0 to 360°), contrast (0 to 100%), spatial frequency (0.2 to 4 cycles per degree), and size (0.2 to 10°), individual parameters were increased in 10- to 15-step increments while all other parameters were held constant. Once optimal stimulus parameters were determined, optimal gratings were presented for 2 s per trial, to determine the precise time (the time of peak response to the periodic stimulus) to deliver electrical stimulation (see above). Finally, neurons were recorded while animals performed the attention task. Gratings drifted at 4 Hz and were of optimal orientation, spatial frequency and approximately two to four times the size of the receptive field to accommodate small shifts in eye position (less than 0.35°). Grating contrast was 70% for putative parvocellular-recipient neurons and between 10 and 25% for putative magnocellular-recipient neurons. For recording sessions in which multiple neurons were recorded simultaneously using the multi-electrode array, gratings parameters were set to stimulate the maximum number of cells as optimally as possible and grating sizes were set to cover the receptive fields of all recorded neurons (never greater than 2°, as receptive-field locations always overlapped greatly). If putative magnocellular- and parvocellular-recipient neurons were recorded simultaneously, grating contrast was set to an intermediate value of approximately 40 to 50%. For the contrast-change detection portion of the attention task, contrast always increased by 10% of the starting contrast.

Data analyses. All recorded spikes were sorted offline using principal components analysis (Spike2 software standard algorithms). Recordings were made from 161 neurons in V1, of which 61 neurons were identified as TCR neurons based on responses during collision testing. Out of these 61 TCR neurons, 22 were recorded with single electrodes (15 from monkey B, 7 from monkey O), and 39 were recorded with the multi-electrode array (30 from monkey B, 9 from monkey O). Twenty-nine additional neurons were classified as putative TCR neurons in multi-electrode recordings (21 from monkey B, 8 from monkey O) based on shock-evoked responses during the attention task. For these neurons, shock-evoked postsynaptic responses were not consistent during collision testing because the shock current was set to accommodate the activity of a different, identified neighbouring TCR in the same recording session. However, during the attention task, shocks systematically evoked postsynaptic spikes at fixed latencies consistent with monosynaptic responses. As TCR neurons and putative TCR neurons did not differ significantly from each other in their percentages of synchronous evoked spikes in attend-towards or attend-away conditions ($P > 0.2$), both groups of neurons were included in subsequent analyses of synchronized and correlated spiking across attention conditions (see below). Receptive fields for all recorded TCR neurons were located in the lower left visual hemifield at parafoveal eccentricities. There were no differences in physiological response properties or attentional modulation of neurons recorded in the two monkeys, and thus, neurophysiological data from both monkeys were combined for all analyses.

TCR neurons were designated as magnocellular- or parvocellular-recipient neurons by their C_{50} values (contrast that evoked a half-maximum response) measured from exponential fits to their contrast–response functions. Magnocellular-recipient neurons ($n = 36$) were classified as neurons with C_{50} values of less than 30% and parvocellular-recipient neurons ($n = 25$) were classified by C_{50} values of greater than 30%. All neurons were classified as simple or complex cells based on the ratio of the first Fourier coefficient (f1) to mean (f0) response, where simple cells have f1:f0 > 1 and complex cells have an f1:f0 < 1 (ref. 33). Mean f1:f0 ratios were: magnocellular-recipient neurons, 0.4 ± 0.04; parvocellular-recipient neurons, 1.2 ± 0.06 ($P < 0.001$). Subsequent analyses of firing rates for visual physiological characterizations and attention-index calculations were performed on the f1 (simple cells) or mean (complex cells) response of each neuron. Orientation-tuning bandwidth was determined by calculating the peak half-width at half-height of Gaussian fits to individual orientation-tuning curves.

Firing rates were measured during inter-trial intervals and during fixation before the presentation of gratings during the attention task. There were no significant differences between magnocellular and parvocellular-recipient neurons or across attention conditions for these firing-rate measurements ($P > 0.7$). Firing rates were also measured during visual-stimulus presentation before the contrast change during attention trials. Magnocellular-recipient neurons had significantly higher firing rates during this period ($P < 0.05$; mean $= 246 \pm 19$ spikes per s) compared to parvocellular-recipient neurons (mean $= 185 \pm 23$ spikes per s), but firing rates assessed over this period for both magnocellular- and parvocellular-recipient neurons did not differ between attend-towards and attend-away conditions ($P > 0.75$).

For all analyses involving an examination of changes in the percentage of shock-evoked spikes, trials were sorted according to whether or not a spike occurred at the specific and fixed postsynaptic spike latency for each individual TCR neuron. Shock-evoked postsynaptic spikes were determined using a 2-ms window aligned by the spike latency for the neuron under study. The proportions of shocks that evoked a postsynaptic spike in each attention condition were determined for each TCR neuron. We also calculated the proportion of non-shock trials in which a spike occurred at the same latency for each attention condition to allow for a comparison between the number of spikes within the latency window with and without electrical stimulation (Supplementary Fig. 1b). As expected, shocks elicited significantly more spikes at the postsynaptic response latency compared to the number of spikes that occurred in the same time window during non-shock trials for the attend-towards condition ($P < 0.01$). However, there were no differences in the number of spikes that occurred at the postsynaptic response latency between non-shock and shock trials for the attend-away condition.

For each TCR neuron, an attention-index value was calculated as the difference (attend towards–attend away) divided by the sum (attend towards + attend away) of average spiking activity over a specified duration of visual stimulation and always before the earliest opportunity for contrast change in attention trials. Importantly, attention-index value calculations always included the time windows corresponding to the shock and shock-evoked postsynaptic responses (which occurred between 1,000 and 1,200 ms in all trials). We calculated attention-index values over long and short durations of visual stimulation: 0 to 1,200 ms, 600 to 1,200 ms, 850 to 1,200 ms, and 1,000 to 1,200 ms after the onset of grating stimulation. When we calculated attention-index values based on the firing rate over long durations (0 to 1,200 ms and 600 to 1,200 ms after grating presentation), we observed no changes in attention index across attention conditions (Supplementary Fig. 1c). When we calculated attention index over short durations (850 to 1,200 ms and 1,000 to 1,200 ms), we observed very small shifts in attention index for magnocellular-recipient neurons only. We compared attention-index values for short durations to spike efficacy values and observed no relationship between overall changes in firing rate with attention and changes in spiking efficacy with attention (Supplementary Fig. 1d).

To examine the influence of attention on the temporal precision of thalamocortical communication across our sample of recorded TCR neurons, we aligned the ongoing spiking responses of each TCR before and after individual shocks, so that time = 0 corresponded to the time when the TCR neuron was expected to produce a shock-evoked postsynaptic response (determined from the shock-evoked postsynaptic latency). This allowed for averaging of spiking activity (or differential spiking activity: activity in attend-towards trials minus activity in attend-away trials) across magnocellular- and parvocellular-recipient neurons with different feedforward spike latencies. To assess the jitter in postsynaptic spike timing across attention conditions, we also plotted time courses surrounding shocks separately for each attention condition (Supplementary Fig. 2a). To demonstrate differential spiking activity for magnocellular- and parvocellular-recipient neurons, we reported two times the standard deviation of average spiking activity before the shock. In all cases, error ranges were reported as standard errors of the mean. We also separated magnocellular- and parvocellular-recipient neurons into two subpopulations based on the presence of a negative dip in spiking activity just before the postsynaptic spike (15 magnocellular-recipient and 10 parvocellular-recipient neurons displayed negative dips). TCR neurons were classified as 'dip' neurons when differential spike count values at –2 or –1 ms time points (relative to the time of the shock-evoked monosynaptic spike) were less than two times the standard deviation of the mean activity before the shock. There was no relationship between spike latency and whether or not a neuron displayed a dip ($P > 0.75$). Moreover, across the sample of dip neurons, there was a range of spike latencies, including latencies longer than the period of the dip, indicating that dips were not systematically a consequence of the shock-induced stimulus artefact obscuring our ability to detect spikes. Supplementary Fig. 2a, b illustrates spiking activity surrounding the postsynaptic spike for dip and no-dip TCR subpopulations (with magnocellular- and parvocellular-recipient groups plotted separately in Supplementary Fig. 2b). We fit Gaussian equations to positive peaks (corresponding to shock-evoked postsynaptic spikes) for dip and no-dip population average curves in order to calculate the width at half-height values for each fit.

During 18 sessions (13 from monkey B, 5 from monkey O) we used a five-channel multi-electrode array with independently movable microelectrodes (Thomas Recording Mini-Matrix system) and recorded from 39 TCR neurons and 29 putative TCR neurons (see above). In 3 of the 18 sessions we recorded from a single TCR neuron. Sessions with paired recordings were as follows: 3 sessions with 1 pair, 1 session with 2 pairs, 2 sessions with 3 pairs, 1 session with 4 pairs, 1 session with 5 pairs, 2 sessions with 6 pairs, 3 sessions with 7 pairs, and 2 sessions with 9 pairs (total = 71 pairs across 15 sessions; mean = 3.3 cells recorded per session). Out of the total 71 pairs, 25 received common input (that is, cross-correlograms contained a central

narrow peak at time = 0) and 46 received independent input. We examined all 50 of the possible common input pairings (in both directions) and used 45 pairings for the analysis of attentional modulation of correlated inputs for pairs receiving common presynaptic input (5 pairings were excluded for lack of sufficient spikes and/or noisy correlograms). To determine whether recording sessions with several pairs did not systematically bias the results, we compared attentional modulation of correlated spikes across recording sessions with greater than 2 pairings and found no differences in attentional modulation of correlated spikes across sessions ($P > 0.05$). We recorded a total of 48 magnocellular–magnocellular pairs (21 received common input, 27 received independent input); a total of 11 parvocellular–parvocellular pairs (2 received common input, 9 received independent input); and a total of 12 magnocellular–parvocellular pairs (2 received common input, 10 received independent input).

We calculated the probability that shocks would evoke synchronous spikes in both TCR neurons across attention conditions. Importantly, our criteria for defining synchronous spikes were strict. Trials with synchronous spikes were those where each TCR neuron fired a shock-evoked postsynaptic spike at its identified postsynaptic spike latency ($n = 71$ pairs).

Cross-correlation analysis was used to determine whether pairs of TCR neurons received input from independent (that is, separate) LGN axons or input from common LGN axons with presumed anatomical divergence. Cross correlations were calculated on a trial-by-trial basis for each of the 71 TCR pairings using spiking data from the 600- to 1,200-ms period of visual stimulation. Shuffled cross correlations were also calculated for each pairing by correlating spikes from neuron A shifted by one stimulus cycle (250 ms) compared to those of neuron B. For each trial, the shuffled correlogram was subtracted from the original correlogram. By employing trial-specific shuffle corrections, we eliminated spike correlations emerging from slow co-variations in neuronal firing rate[34] and co-activation from a common visual stimulus (stimulus-dependent correlations). Shuffle-subtracted correlograms were reported as average percentages of total spikes for each attention condition.

Out of 71 pairs of simultaneously recorded TCR neurons, 25 pairs (17 from monkey B, 8 from monkey O) displayed narrow peaks (<3 ms) in their cross correlograms, centred at time zero, indicating the pair received common presynaptic input, presumably from feedforward axons with branches that contacted both neurons. In addition to magnocellular–magnocellular ($n = 21$) and parvocellular–parvocellular pairs ($n = 2$), we also encountered mixed magnocellular–parvocellular pairs ($n = 2$) receiving common input. Neurons in mixed magnocellular–parvocellular-recipient pairs were located within close proximity to one another in cortical depth (within 75 μm), and tended to display similar contrast sensitivity and/or orientation selectivity, suggesting that neurons in these mixed pairs were both located near the laminar border between layers 4Cα and 4Cβ.

For the analysis of attentional modulation of TCR pairs receiving common input, we calculated the difference in peak area, measured in 3 bins of 1-ms width centred at time = 0, between shuffle-corrected cross-correlograms in each attention condition. Cross-correlogram peak heights in each attentional condition corresponded to roughly 3% of total spikes (Fig. 4c) and the average attention-mediated reduction in peak height across all cells was $-0.3 \pm 0.2\%$ suggesting that attention caused a 10% reduction in correlated spiking resulting from divergent input from a common presynaptic source.

To compare actual measured percentages of synchronous shock-evoked postsynaptic spikes to predicted percentages, we compared the measured incidences of synchronous spikes (as described above) with the product of each individual neuron's probability of firing a postsynaptic spike in response to the shock (for example, Fig. 2d). We then calculated the difference (actual – predicted) in the occurrence of synchronous spikes for common input TCR pairs and independent-input TCR pairs across attention conditions.

Approximation of overall attentional modulation of signal-to-noise ratio was calculated as: (change in percentage signal)/(change in percentage noise), which translates to (1 + average percentage increase in shock-evoked synchronized spikes)/(1 – average percentage decrease in synchronized spikes in cross-correlogram peaks). The average percentage increase in shock-evoked synchronized spikes = 8%, and average percentage decrease in synchronized spikes in cross-correlogram peaks = 10% for the population of recorded TCR pairs (see above).

Statistics. Parametric or non-parametric comparisons tests (*t*-test or rank-sum test, respectively) were used for all two-sample comparisons depending on the distribution normality of the samples tested. To test for distribution normality, one-sample Kolmogorov–Smirnov tests were used. To examine whether any given distribution of data differed from an equivalent normal distribution, the sample distribution was compared to a normal distribution with the same standard deviation as the sample. Accordingly, the Kolmogorov–Smirnov test compared a sample distribution to a proposed continuous distribution defined by the same range and variance parameters as the sample.

31. Briggs, F. & Usrey, W. M. A fast, reciprocal pathway between the lateral geniculate nucleus and visual cortex in the macaque monkey. *J. Neurosci.* **27,** 5431–5436 (2007).
32. Briggs, F. & Usrey, W. M. Parallel processing in the corticogeniculate pathway of the macaque monkey. *Neuron* **62,** 135–146 (2009).
33. Skottun, B. C. *et al.* Classifying simple and complex cells on the basis of response modulation. *Vision Res.* **31,** 1078–1086 (1991).
34. Brody, C. D. Slow covariations in neuronal resting potentials can lead to artefactual fast cross-correlations in their spike trains. *J. Neurophysiol.* **80,** 3345–3351 (1998).